pubs.acs.org/acschemicalbiology

Letters

Ceramide-1-Phosphate Is Involved in Therapy-Induced Senescence

Alec Millner, Logan Running, Nicole Colon-Rosa, Diana S. Aga, Jonna Frasor,* and G. Ekin Atilla-Gokcumen*

Cite This: *ACS Chem. Biol.* 2022, 17, 822–828

Read Online

ACCESS | Metrics & More | Article Recommendations | Supporting Information

ABSTRACT: Sphingolipids are key signaling lipids and their dysregulation has been associated with various cellular processes. We have previously shown significant changes in sphingolipids in therapy-induced senescence, a state of cell cycle arrest as a response to chemotherapy, including the accumulation of ceramides, and provided evidence suggesting that ceramide processing is important for this process. Herein, we conducted a focused small molecule inhibitor screen targeting the sphingolipid pathway, which highlighted a new lipid regulator of therapy-induced senescence. Among the inhibitors tested, the inhibition of ceramide kinase by NVP-231 reduced the levels of senescent cells. Ceramide kinase knockdown exhibited similar effects, strongly supporting the involvement of ceramide kinase during this process. We showed that ceramide-1-phosphate was upregulated in therapy-induced senescence and that NVP-231 reduced ceramide-1-phosphate levels in different cell line models of therapy-induced senescence. Finally, ceramide-1-phosphate addition to NVP-231-treated cells reversed the effects of NVP-231 during senescence. Overall, our results identify a previously unknown lipid player in therapy-induced senescence and highlight a potential targetable enzyme to reduce the levels of therapy-induced senescent cells.

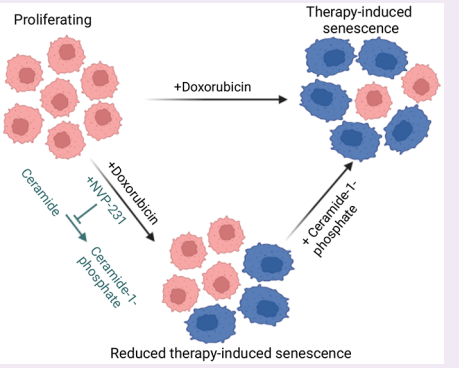

Sphingolipids and their metabolites have emerged as important signaling molecules involved in various fundamental cellular processes and diseases. Although all sphingolipids share a common sphingosine backbone, they achieve high structural diversity through incorporation of acyl chains with various length and attachment of different headgroups to the sphingosine backbone. Ceramide, the central molecule of the sphingolipid pathway, is synthesized from palmitoyl CoA and serine by a network of enzymes, which are tightly regulated. Ceramide can be used as a building block to produce other sphingolipids, including sphingomyelin, glycosphingolipids, and ceramide-1-phosphate (C1P, reviewed in ref 1).

Ceramide levels are regulated by *de novo* synthesis, conversion to or breakdown of sphingomyelin or glycosphingolipids, or breakdown of ceramide into sphingosine. Cells' ability to regulate sphingolipid metabolism is crucial for homeostasis, as dysregulation of sphingolipid-processing enzymes can lead to increased cell growth, inflammation, and cell death. Many chemotherapeutic strategies affect sphingolipid levels, and alterations to the sphingolipid landscape has been correlated with therapy resistance. Primarily, transformations that affect the levels of pro-death (i.e., ceramides) and pro-survival (i.e., sphingosine-1-phosphate and C1P) sphingolipids have been linked to chemotherapy resistance.[2]

Many chemotherapeutic agents induce DNA damage and cause cell death. However, DNA damage can also induce permanent growth arrest, known as therapy-induced senescence (TIS).[3] Senescent cells have been shown to promote cancer growth and other adverse effects, including inflammation, reducing overall treatment effectiveness.[4] The details on how senescent cells achieve their characteristic growth arrest remains largely unknown. Previous studies have reported increased lipid metabolism[5] and sphingolipid levels[6,7] during TIS. However, there is a gap in understanding of the biochemical machineries that regulate lipid levels and their functional involvement in TIS. Identification of lipid-related enzymes that are responsible for modulating lipid levels during this process may provide insight into how cells achieve and maintain senescence and provide potential targets to prevent or reduce therapy-induced senescence.[8]

Toward identifying new lipid players of TIS, we have previously conducted the first untargeted lipidomics investigations during doxorubicin-induced (Dox-induced) senescence and identified the depletion of 1-deoxyceramides as a key lipid-related change of this process.[6] Although 1-deoxyceramides do not have any known signaling roles, changes in their levels can mediate sphingolipid remodeling, since deoxyceramides act as metabolic "sinks" for sphingolipid

Received: March 11, 2022
Accepted: March 23, 2022
Published: March 30, 2022

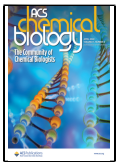

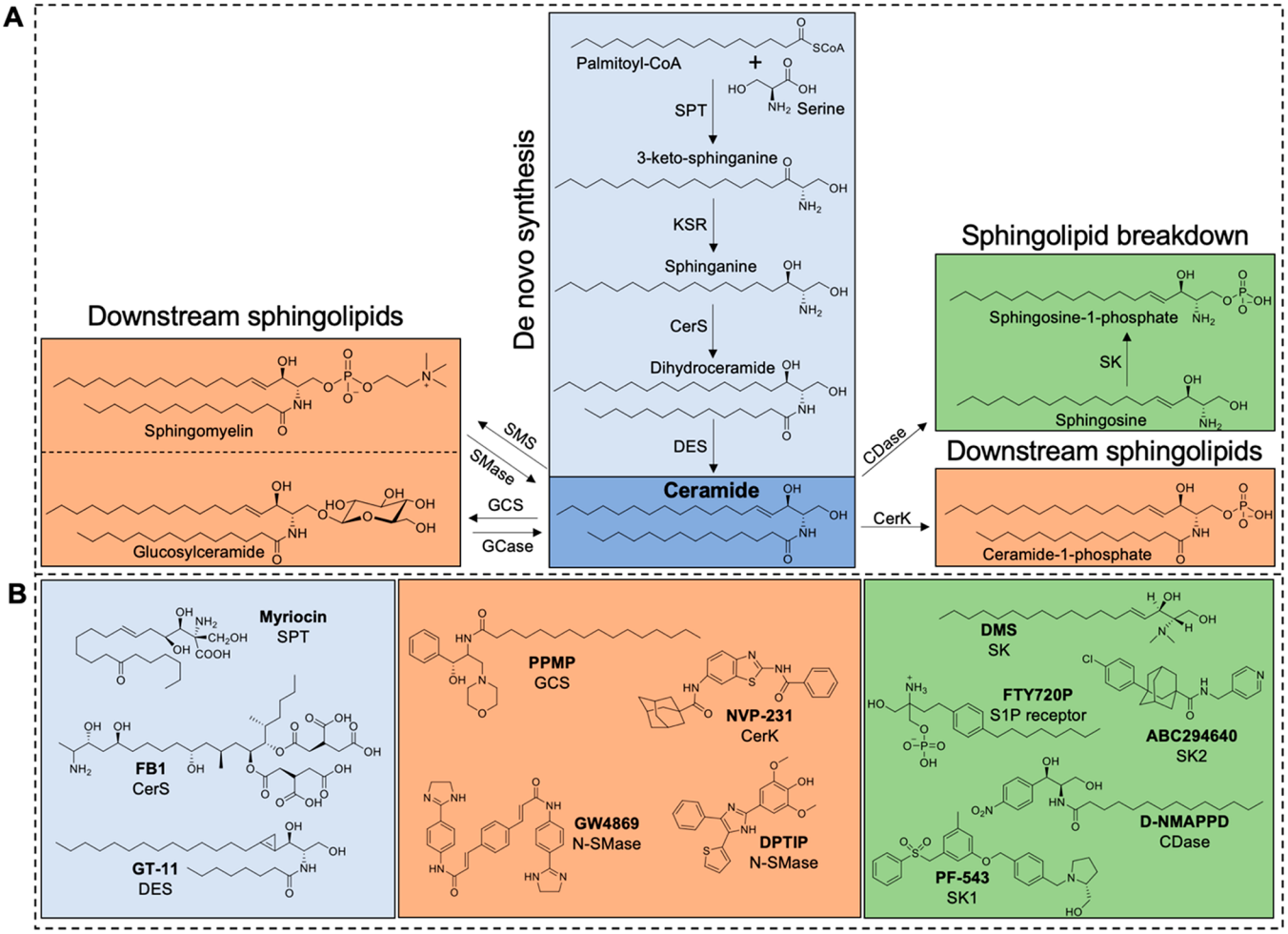

Figure 1. Small molecule inhibitors of sphingolipid pathway. (A) Simplified diagram of sphingolipid synthesis. Sphingolipids containing a C14:0 fatty acid are shown as examples. Ceramide, highlighted in dark blue, is central to the sphingolipid pathway. Ceramide can be synthesized *de novo* (light blue), incorporated into other downstream sphingolipids (orange), or broken down into sphingosine (green). (B) Small molecule inhibitors used. Inhibitors are categorized based on their target's role in the sphingolipid pathway.

processing: they cannot be converted to downstream sphingolipid products, including sphingomyelins, glucosylceramides, and ceramide- and sphingosine-1-phosphate due to the lack of a 1′-OH moiety.[9] We were able to decrease the levels of senescent cells by increasing the levels of deoxyceramides,[6] which suggested potential involvement of a sphingolipid(s) that is downstream of ceramide processing. In this study, we took a small molecule approach to identify sphingolipid species that are affected by lipid modeling and that might be functionally involved in TIS. We investigated the effect of inhibitors that target biosynthesis and degradation of sphingolipids and found that inhibition of ceramide kinase (CerK) resulted in significant reduction in senescence. Subsequent lipidomic analysis showed that the inhibition of CerK decreases the levels of C1P but does not affect the levels of other sphingolipids. We also showed that CerK inhibition reduced senescence levels in multiple cell line models and can be overcome by supplementing cells with C1P. Overall, our results for the first time link C1P to TIS and suggest that decreasing the levels of C1P can reduce TIS.

RESULTS AND DISCUSSION

Inhibition of CerK Affects TIS. Sphingolipids have been shown to play crucial roles in various cellular processes, including cell proliferation, survival, and death.[1] To probe the involvement of different lipid-related enzymes and their products in TIS, we used a focused small molecule library. Ceramides can accumulate via increased *de novo* synthesis, decreased breakdown into sphingosine, or disruption of the synthesis or salvage of downstream sphingolipids[1] (Figure 1A). Based on literature surveys, we identified 12 small molecule inhibitors that target various biosynthetic and breakdown steps in the sphingolipid pathway (Figure 1B, Table S1).

For targeting *de novo* synthesis of ceramide, we used myriocin, FB1, and GT-11 which inhibit serine palmitoyl transferase, ceramide synthase, and dihydroceramide desaturase, respectively. These inhibitors of *de novo* ceramide synthesis are potent, with IC_{50} = 1−100 nM,[10,11] and have been used extensively to downregulate ceramide production (Table S1). We also used D-PPMP, GW4869, DPTIP, and NVP-231 to target the production of downstream sphingolipid-related enzymes, glucosylceramide synthase, neutral sphingomyelinase, and ceramide kinase, respectively.[11−14] Finally, D-NMAPPD, dimethylsphingosine, PF-543, ABC294640, and FTY720P were used to inhibit acid ceramidase, sphingosine kinase 1 and 2, and a sphingosine-1-phosphate receptor, respectively.[15−18]

https://doi.org/10.1021/acschembio.2c00216
ACS Chem. Biol. 2022, 17, 822−828

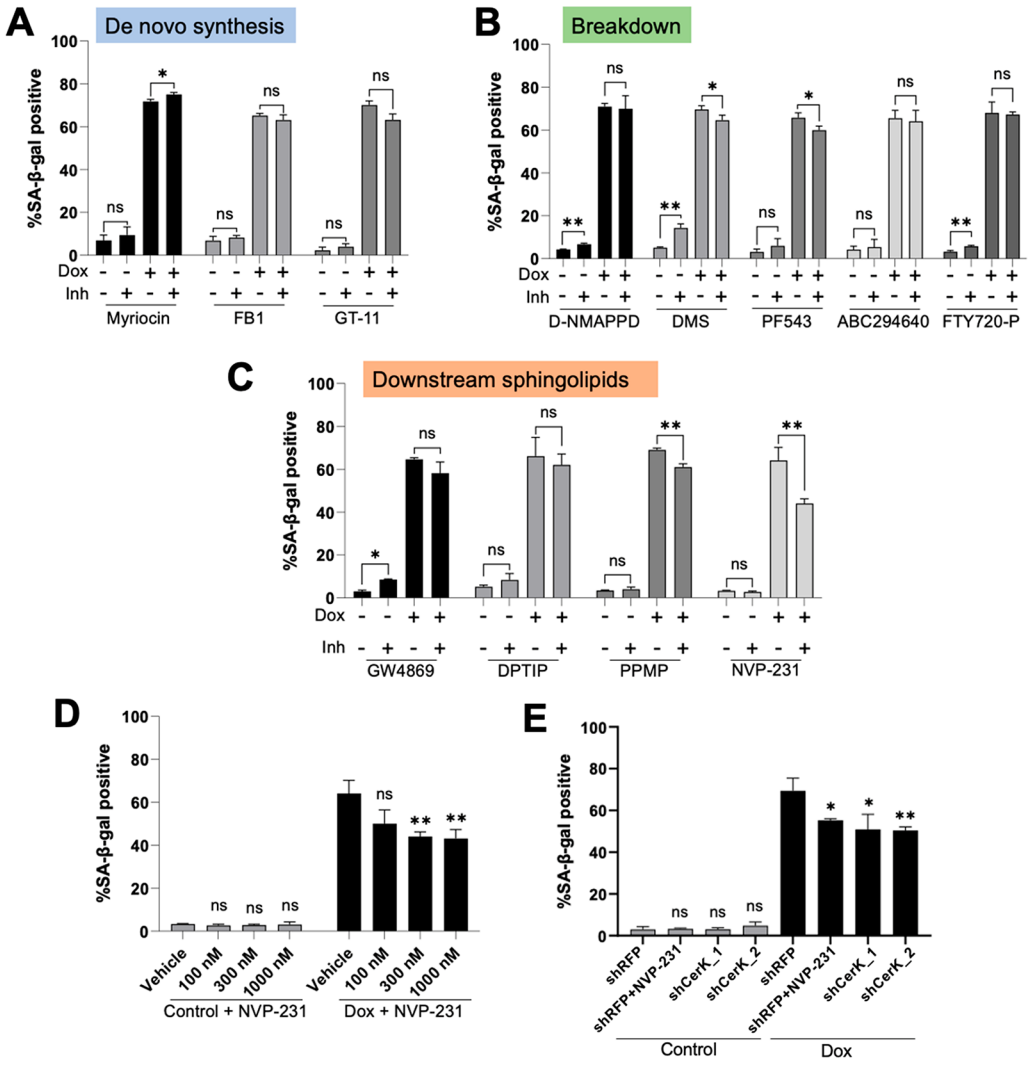

Figure 2. Inactivation of CerK significantly desensitizes cells to TIS. Measurement of SA-β-gal cells in control and doxorubicin (Dox)-treated HCT-116 cells in the presence (300 nM) or absence of inhibitor (Inh). (A) Inhibitors for *de novo* synthesis of ceramide (myriocin, FB1, and GT-11) did not show a profound effect on SA-β-gal levels compared to Dox-treated cells without inhibitor treatment. (B) Inhibitors of ceramide breakdown (D-NMAPPD, DMS, PF543, ABC294640, and FTY720-P) did not show a profound effect on SA-β-gal levels compared to Dox-treated cells without inhibitor treatment. (C) Inhibitors of downstream sphingolipids. GW4869, DPTIP, and PPMP did not show profound effects on SA-β-gal levels compared to Dox-treated cells. NVP-231 resulted in 44% positive SA-β-gal cells as compared to 64% positive SA-β-gal cells in Dox-treated cells. (D) Dose–response effect of NVP-231. Inhibitors were supplemented at the time of Dox-treatment and during the recovery period. (E) TIS in shCerK cell lines. CerK was inactivated in HCT-116 cells using lentiviral shRNA vectors. Two constructs were used, resulting in shCerK_1 and shCerK_2 cell lines. Compared to a nontarget (Red Fluorescent Protein, shRFP) control, the levels of senescent cell in shCerK_1 and shCerK_2 cell lines were reduced. Measurements were done at least in triplicate ($n = 3$), counting 200 cells per replicate. Data shown as mean ± standard deviation, * $p < 0.05$, ** $p < 0.01$.

To investigate the effect of these small molecule inhibitors on senescence, we induced TIS as we established previously.[6] Briefly, HCT-116 cells, a human colorectal cancer cell line, were treated with doxorubicin (Dox) for 24 h. After Dox-treatment, the treatment media was removed and replaced with fresh growth medium. Cells were then cultured in growth medium for an additional 72 h, which we will refer to as the recovery period. The senescence levels were assessed using senescence-associated-β-galactosidase (SA-β-gal) activity assay.[6] As we expected, Dox treatment resulted in ∼70% of cells exhibiting increased SA-β-gal activity (Figure 2 and Figure S1A) and increased p21 levels (Figure S1B). To determine the effect that sphingolipid inhibition has on TIS, we measured SA-β-gal activity with various small-molecule inhibitors supplementing the treatment. Specifically, we introduced the small molecule inhibitors at the same time with Dox and included a fresh dose during the recovery period (see Supporting Information for detail and Figure S2). We used these compounds at low concentrations (100 nM to 1 μM) due to their established potencies and the prolonged treatment times (Figures 2 and S2) in order to avoid any cytotoxic effects that might be due to the compound treatment only. At 1 μM, some inhibitors modestly affect the senescence levels in the absence of Dox treatment (Figure S2). This is most likely due to the fact that these inhibitors can impact ceramide levels, the accumulation of which has been linked to senesecence.[5,6,19] Figure 2 shows the results from 300 nM inhibitor treatments in the presence and absence of Dox. Inhibition of *de novo* ceramide biosynthesis by myriocin, FB1, and GT-11 (Figure 2A) or breakdown (Figure 2B) of ceramides by D-NMAPPD,

https://doi.org/10.1021/acschembio.2c00216
ACS Chem. Biol. 2022, 17, 822–828

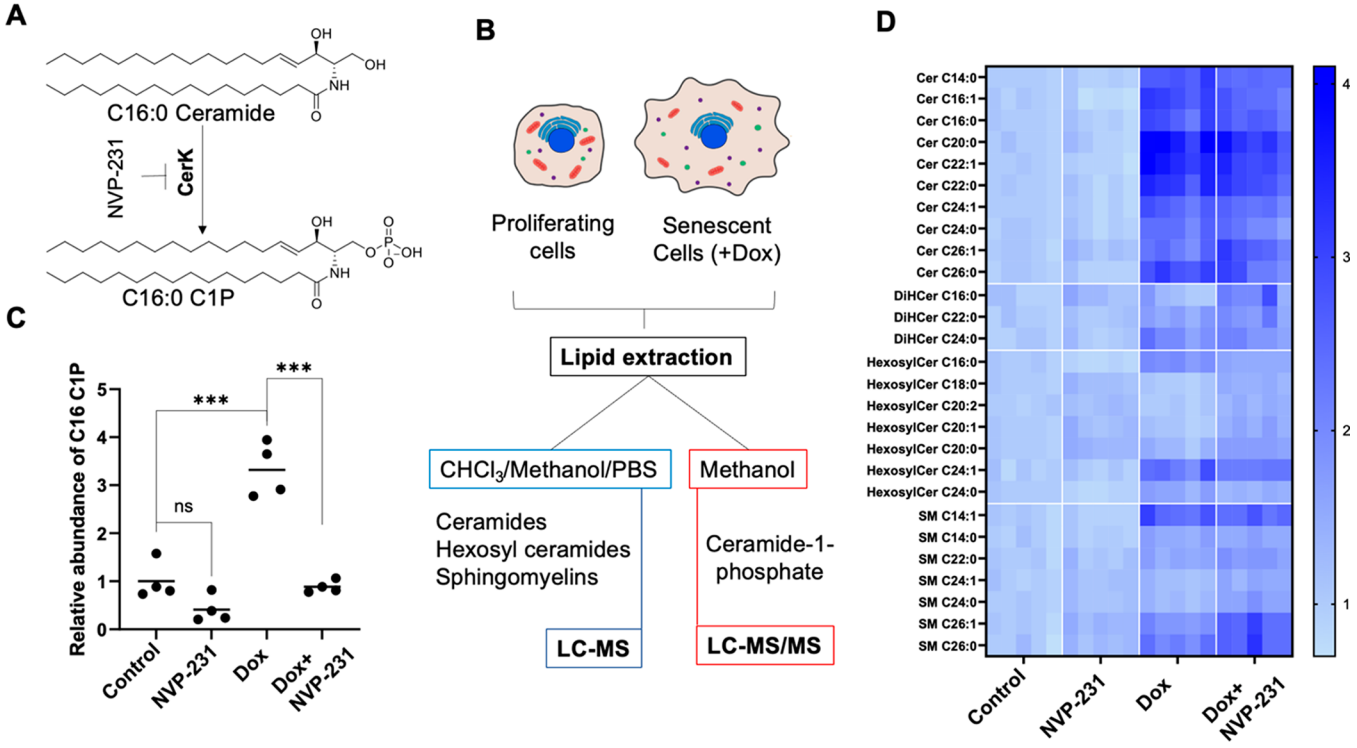

Figure 3. Sphingolipid extraction methods and C1P analysis. (A) NVP-231 targets CerK, inhibiting C1P synthesis. C16:0 ceramide and C16:0 C1P are shown. (B) Extraction and analysis methods for C1P and other sphingolipids. (C) Relative abundance of C16:0 C1P levels in control, doxorubicin (Dox)-treated cells, and the corresponding NVP-231 treated cells. Four biological replicates were used for each condition. C16:0 C1P levels were corrected to C8:0 C1P internal standard. To determine relative abundance, the corrected abundance of C16:0 C1P in each replicate was divided by the average abundance of C16:0 C1P in control. ***$p < 0.001$. (D) Relative abundance of sphingolipids in control and Dox-treated cells treated with NVP-231. Five biological replicates were used for each condition. The total carbon number of the acyl chain and degree of unsaturation are listed. Internal standards were used for correction; C17:0 ceramide for ceramides and dihydroceramides, C17:0 glucosylceramide for hexosylceramides, and C17:0 sphingomyelin for sphingomyelins. To determine relative abundance, the corrected abundance of each lipid species was divided by the average corrected abundance of the species in the control samples.

ABC294640, and FTY720-P did not have a significant effect on senescence levels. Similarly, blocking ceramide production by inhibiting neutral sphingomyelinase (by GW4869 or DPTIP) did not have a strong effect on senescence (see Figure S2 for dose-dependent effects). However, DMS, PF-543, PPMP, and NVP-231 resulted in a statistically significant reduction of SA-β-gal positive cells during Dox treatment ($p < 0.05$, 5−30% reduction, Figure 2B−C). Among these inhibitors, we decided to focus on NVP-231, which had the strongest effect on senescence. Blocking the phosphorylation of ceramide into C1P by inhibiting ceramide kinase (CerK) using NVP-231 showed a concentration dependent decrease of senescent cells (~30% reduction in SA-β-gal positive cells at 300 nM and 1 μM; Figure 2D and Figure S1A) and downregulation of p21 (Figure S1B). To confirm the role of CerK in TIS, we knocked down CerK using two lentiviral shRNA constructs (see Methods) and investigated the effect of Dox in these cell lines. We used shRFP, a nontarget lentiviral construct, as a negative control. CerK knockdown (Figure S3) resulted in reduced levels of senescent cells after Dox treatment (Figure 2E), strongly supporting the role of CerK during this process.

After confirming the involvement of CerK in Dox-induced senescence in HCT-116 cells, we tested the effect of NVP-231 in two additional models of TIS to assess the generalizability of the effect of NVP-231 during TIS. Following the same experimental setup described above, we first induced TIS using Dox in HT-29 cell lines and investigated the effect of CerK inhibition on the levels of senescence cells (Figure S4). Second, to test if the observations above are specific to Dox-induced senescence, we investigated the effect of CerK inhibition in senescence levels during etoposide-induced senescence in HCT-116 cells (Figure S5). In both of these models, NVP-231 had similar effects, significantly reducing the levels of senescent cells ($p < 0.05$, Figure S4A for Dox-induced senescence in HT-29 cells; Figure S5A for etoposide-induced senescence in HCT-116 cells). Overall, our results suggest that the effect of NVP-231 on TIS is not specific to a particular chemotherapeutic agent or a cell line but rather can be generalized as a phenomenon associated with TIS.

Ceramide-1-Phosphate Accumulates During TIS. Our results show that pharmacological and genetic inactivation of CerK reduce the levels of senescence cells. CerK is a lipid kinase that catalyzes the phosphorylation of ceramide at the 1-hydroxyl position, forming C1P (Figure 3A), an important signaling molecule that has been reported to have mitogenic, pro-survival, and inflammatory roles.[20] In order to probe C1P's potential involvement in TIS, we developed a method to extract and measure C1P levels in cells. Instead of a commonly used chloroform-based biphasic extraction method for sphingolipids, we utilized a monophasic methanol extraction due to the hydrophilic nature of C1P as compared to other sphingolipids (Figure 3B). This methanol extraction resulted in high C1P recovery (84.2 ± 10.2%; see Supporting Information for details). Using this method, we extracted C1P from proliferating and senescent cells. After normalization based on protein content, samples were analyzed using LC-

https://doi.org/10.1021/acschembio.2c00216
ACS Chem. Biol. 2022, 17, 822−828

MS/MS (see Methods for full detail). Briefly, C16:0 C1P levels were measured in positive ionization mode, using C8:0 C1P as an internal standard. We note that C16:0 C1P was the only ceramide-1-phosphate species we detected in lysates. Multiple reaction monitoring transitions for C8:0 C1P and C16:0 C1P were m/z 506.4/264.2 and 618.5/264.2 for quantifier ions, and 506.4/455.9 and 618.5/600.6 for qualifier ions, respectively. We found that C16:0 C1P is upregulated in Dox-induced senescence in HCT-116 cells, showing a 3-fold increase in senescent cells as compared to proliferating cells ($p < 0.05$, Figure 3B). Similarly, C16:0 C1P was also upregulated in additional models of TIS we described earlier (Figure S4B and Figure S5B).

Inhibition of CerK Significantly Lowers C1P Levels. The effects observed from inhibition of CerK with NVP-231 (Figure 3A) could potentially be due to increased levels of substrate (ceramide) or decreased levels of product (C1P). To understand how NVP-231 affects the sphingolipidome, we measured C1P levels and other sphingolipids (Figures 3, S4, and S5) in proliferating and senescent cells. NVP-231 treatment resulted in a modest decrease in C1P levels in control cells. However, NVP-231 treatment has a strong effect in Dox- and etoposide-treated senescent cells and caused ~3.5-fold reduction in C1P levels ($p < 0.001$, Figure 3C; $p < 0.05$, Figure S4B; and $p < 0.001$, Figure S5B). Investigating the levels of other sphingolipids after NVP-231 treatment using our previously established LC-MS based measurements[6] (Figure 3B, and see Supporting Information for details) showed that there were no appreciable changes in the levels of ceramides, dihydroceramides, sphingomyelins, and hexosylceramides upon NVP-231 treatment (Figures 3D, S4C, and S5C). These results show that NVP-231 treatment in senescence primarily decreased the levels of the lipid product, C1P, without causing any significant changes in the levels of other sphingolipids, suggesting that C1P is involved in senescence. To assess the involvement of C1P in the reduction of senescence we observed with NVP-231 treatment, we carried out a C1P addback experiment, wherein we supplemented NVP-231 treatment with C8:0 C1P (Figure 4) which exhibits similar bioactivity to C16:0 C1P but has a better solubility.[21,22] C8:0 C1P treatment alone did not affect SA-β-gal; however, when it was added with NVP-231, senescence levels were increased, reversing the effect of NVP-231 in TIS.

In summary, in this work, motivated by our previous findings on the involvement of 1-deoxyceramides, we employed a pharmacological approach to identify functional sphingolipids during TIS. 1-Deoxyceramides are noncanonical ceramide species and may act as competitive inhibitors for ceramide processing enzymes due to the 1′-OH moiety.[9] Our results show that C1P, a ceramide product, is upregulated in TIS and that blocking its production by inhibiting CerK reduces the levels of senescent cells in multiple models of TIS. We also show that the effect of CerK inhibition can be overcome by adding C1P back in the growth media, directly linking the activity of CerK and increased levels of C1P to establishing and maintaining TIS. However, we should note that whether the changes in C1P levels act as a signal on its own or result in changes in the sphingolipid landscape which mediates senescence is to be elucidated.

Upregulation of C1P could potentially promote cell survival through various mechanisms. C1P has been shown to inhibit cell death by blocking A-SMase[23] and SPT[24] or by upregulation of other key enzymes, including the anti-

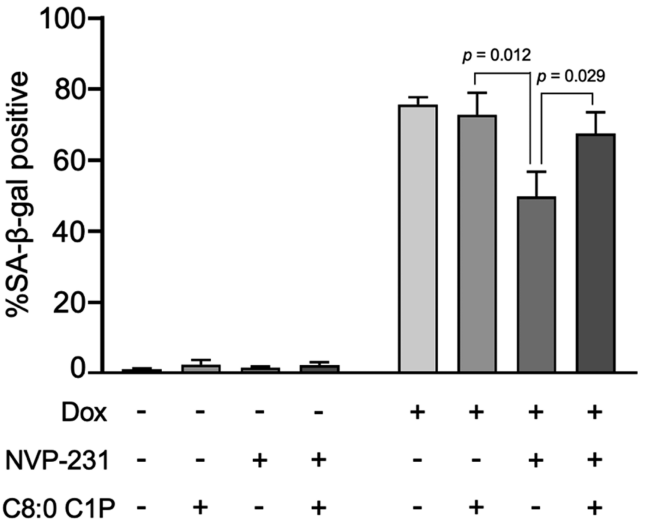

Figure 4. C1P addback reverses the effect of NVP-231 during senescence. Measurement of SA-β-gal-positive cells in control and doxorubicin (Dox)-treated HCT-116 treated with NVP-231 and C8:0 C1P. C8:0 C1P and NVP-231 were added to the growth medium at the time of Dox treatment and during the recovery period. C8:0 C1P alone had no effect on SA-β-gal, while NVP-231 alone significantly reduced SA-β-gal. Co-treatment with C8:0 C1P (100 nM) and NVP-231 (300 nM) resulted in an increase of SA-β-gal. Measurements were done in triplicate ($n = 3$), counting 200 cells per replicate. Data shown as mean ± standard deviation.

apoptotic regulator Bcl-X_L.[22] It is possible that cells can reduce the levels of pro-apoptotic ceramides by converting them to C1P, which, in turn, inhibits ceramide production via the mechanisms mentioned above. C1P has also been reported to directly activate cPLA$_2\alpha$, leading to the release of arachidonic acid and pro-inflammatory eicosanoids.[25] Interestingly, interleukin 1β, a pro-inflammatory cytokine commonly associated with the secretory phenotype of senescence,[26] has been shown to increase endogenous C1P levels.[27] Whether C1P plays a pro-survival and anti-apoptotic role or has deleterious pro-inflammatory effects appears to be tissue and context dependent,[20] but many of these roles could potentially be involved in senescence growth arrest and the secretory phenotype. We note that we do not see a complete rescue from senescence when we reduce C1P levels. This is likely due to the fact that C1P is not the only lipid regulator of this process. In addition to protein players associated with senescence, other sphingolipids also regulate this process.[3,5] It has been shown that sphingolipid production is increased during senescence, resulting in higher levels of ceramides during this process ([6,19] and Figure 3D). It is possible that the increased production of C1P we observe is due to the higher levels of its metabolic precursor sphingolipid, ceramide. While its role in TIS is to be determined, C1P can inhibit cell death by blocking sphingolipid production via A-SMase[23] and SPT[24] or activating cPLA$_2\alpha$.[25] As such, it is plausible to envision that C1P functions through multiple axes including transcriptional activation of pro-survival genes or modulating therapy-induced senescence.

METHODS

Lipid Extraction. All sphingolipids, except C1P, were extracted based on previous protocols (see Supporting Information for details).[6] The extraction method for C1P was modified from a previous protocol.[28] Fresh cell pellets were resuspended in 1 mL PBS.

https://doi.org/10.1021/acschembio.2c00216
ACS Chem. Biol. 2022, 17, 822−828

A 30 μL aliquot of this cell suspension was removed and used to determine protein concentration (see Supporting Information for details). The remaining cell suspension was centrifuged again to pellet the cells, and the PBS was removed. Cell pellets were resuspended in 1 mL of cold methanol. The cell−methanol suspension was sonicated at 40% power (three times, 10 s), after which the samples were centrifuged (16,000*g*, 15 min, 4 °C). 900 μL of the supernatant was transferred into a 1-dram vial, being careful to not disturb the pellet. A second extraction was performed by adding 900 μL of methanol to the remaining cell pellet, followed by sonication and centrifugation as before. 900 μL of supernatant was transferred into the same 1-dram vial from the first extraction. The methanol was dried under vacuum. To determine the percentage of C1P recovered with this method, HCT-116 cell pellets were extracted, as described above, spiking with C16:0 C1P before (prespike) or after (postspike) extraction. Percent recovery was calculated as the abundance of C16:0 C1P in the prespike sample divided by the abundance of C16:0 C1P in the postspike sample, resulting in 84.2 ± 10.2% recovery (n = 3) Samples were normalized based on protein concentration and resuspended in methanol ≥120 μL. C17:0 ceramide and C8:0 ceramide-1-phosphate were used as internal standards.

LC-MS Acquisition and Analysis. LC-MS analysis of sphingolipids, except C1P, was performed as described previously.[6] Please see the Supporting Information for details.

LC-MS/MS analysis for C1P was performed using an Agilent 1200 liquid chromatography tower coupled to a Thermo Scientific TSQ Quantum Ultra mass spectrometer. 1 μM standards of C16:0 ceramide, C17:0 ceramide, C8:0 C1P, and C16:0 C1P were prepared in methanol and injected directly to the mass spectrometer by infusion and heated electrospray ionization to optimize source conditions. The parameters were optimized in positive mode as follows: Capillary temperature, 250 °C; vaporizer temperature, 300 °C; sheath gas pressure, 17 arb; aux gas pressure, 4 arb; spray voltage, 4500 V. Separation was achieved using reversed-phase chromatography with a Gemini C18 reversed-phase column (5 μm, 4.6 × 50 mm) with a C18 reversed-phase guard cartridge. The column was operated at 60 °C to reduce carryover. Mobile phase A was 60:39:1 methanol:water:formic acid and mobile phase B was 99:1 methanol:formic acid. Both mobile phases were supplemented with 5 mM ammonium formate. The method began with holding 40% B for 30 s before increasing to 100% B over a 90 s gradient. 100% B was held isocratic for 8 min, followed by equilibration with 40% B for 5 min. Flow rate was set to 1 mL/min. Both C8:0 and C16:0 C1P displayed $[M + H]^+$ as the highest intensity precursor ion. The primary product ion for both C8:0 and C16:0 C1P was m/z 264.2. The secondary product ions were m/z 455.9 and 600.6 for C8:0 and C16:0 C1P, respectively. Limit of detection for C16:0 C1P was ∼1 nM (∼0.6 ng/mL).

■ ASSOCIATED CONTENT

Supporting Information

The Supporting Information is available free of charge at https://pubs.acs.org/doi/10.1021/acschembio.2c00216.

Additional experimental methods, LC-MS-based lipid assignments, table of small molecule inhibitors, and figures for representative images and Western blot for TIS characterization, SA-β-gal assays for full sphingolipid inhibitor screen, CerK knockdown efficiency, NVP-231 studies in doxorubicin-treated HT-29, and NVP-231 studies in etoposide-treated HCT-116 (PDF)

■ AUTHOR INFORMATION

Corresponding Authors

G. Ekin Atilla-Gokcumen − *Department of Chemistry, University at Buffalo, The State University of New York (SUNY), Buffalo, New York 14260, United States;* orcid.org/0000-0002-7132-3873; Email: ekinatil@buffalo.edu

Jonna Frasor − *Department of Physiology and Biophysics, University of Illinois at Chicago, Chicago, Illinois 60612, United States*; Email: jfrasor@uic.edu

Authors

Alec Millner − *Department of Chemistry, University at Buffalo, The State University of New York (SUNY), Buffalo, New York 14260, United States;* orcid.org/0000-0003-1365-2342

Logan Running − *Department of Chemistry, University at Buffalo, The State University of New York (SUNY), Buffalo, New York 14260, United States;* orcid.org/0000-0001-5972-8483

Nicole Colon-Rosa − *Department of Chemistry, University at Buffalo, The State University of New York (SUNY), Buffalo, New York 14260, United States; Department of Chemistry, University of Puerto Rico, Cayey 00736, Puerto Rico*

Diana S. Aga − *Department of Chemistry, University at Buffalo, The State University of New York (SUNY), Buffalo, New York 14260, United States;* orcid.org/0000-0001-6512-7713

Complete contact information is available at: https://pubs.acs.org/10.1021/acschembio.2c00216

Notes

The authors declare no competing financial interest.

■ ACKNOWLEDGMENTS

We gratefully acknowledge the support from National Science Foundation (1817468) and the Department of Defense (BC191366). We also acknowledge summer support for N.C.-R. from National Science Foundation (1852372, REU Site).

■ REFERENCES

(1) Hannun, Y. A.; Obeid, L. M. Sphingolipids and their metabolism in physiology and disease. *Nat. Rev. Mol. Cell Biol.* **2018**, *19* (3), 175−191.

(2) Lewis, A. C.; Wallington-Beddoe, C. T.; Powell, J. A.; Pitson, S. M. Targeting sphingolipid metabolism as an approach for combination therapies in haematological malignancies. *Cell Death Discov* **2018**, *4*, 72.

(3) Ewald, J. A.; Desotelle, J. A.; Wilding, G.; Jarrard, D. F. Therapy-induced senescence in cancer. *J. Natl. Cancer Inst* **2010**, *102* (20), 1536−46.

(4) Wyld, L.; Bellantuono, I.; Tchkonia, T.; Morgan, J.; Turner, O.; Foss, F.; George, J.; Danson, S.; Kirkland, J. L. Senescence and Cancer: A Review of Clinical Implications of Senescence and Senotherapies. *Cancers (Basel)* **2020**, *12* (8), 2134.

(5) Flor, A. C.; Wolfgeher, D.; Wu, D.; Kron, S. J. A signature of enhanced lipid metabolism, lipid peroxidation and aldehyde stress in therapy-induced senescence. *Cell Death Discov* **2017**, *3*, 17075.

(6) Millner, A.; Lizardo, D. Y.; Atilla-Gokcumen, G. E. Untargeted Lipidomics Highlight the Depletion of Deoxyceramides during Therapy-Induced Senescence. *Proteomics* **2020**, *20* (10), No. e2000013.

(7) Modrak, D. E.; Leon, E.; Goldenberg, D. M.; Gold, D. V. Ceramide regulates gemcitabine-induced senescence and apoptosis in human pancreatic cancer cell lines. *Mol. Cancer Res.* **2009**, *7* (6), 890−6.

(8) Ovadya, Y.; Krizhanovsky, V. Strategies targeting cellular senescence. *J. Clin Invest* **2018**, *128* (4), 1247−1254.

(9) Jimenez-Rojo, N.; Sot, J.; Busto, J. V.; Shaw, W. A.; Duan, J.; Merrill, A. H., Jr; Alonso, A.; Goni, F. M. Biophysical properties of novel 1-deoxy-(dihydro)ceramides occurring in mammalian cells. *Biophys. J.* **2014**, *107* (12), 2850−2859.
(10) Wadsworth, J. M.; Clarke, D. J.; McMahon, S. A.; Lowther, J. P.; Beattie, A. E.; Langridge-Smith, P. R.; Broughton, H. B.; Dunn, T. M.; Naismith, J. H.; Campopiano, D. J. The chemical basis of serine palmitoyltransferase inhibition by myriocin. *J. Am. Chem. Soc.* **2013**, *135* (38), 14276−85.
(11) Skacel, J.; Slusher, B. S.; Tsukamoto, T. Small Molecule Inhibitors Targeting Biosynthesis of Ceramide, the Central Hub of the Sphingolipid Network. *J. Med. Chem.* **2021**, *64* (1), 279−297.
(12) Lauer, S. A.; Ghori, N.; Haldar, K. Sphingolipid synthesis as a target for chemotherapy against malaria parasites. *Proc. Natl. Acad. Sci. U. S. A.* **1995**, *92* (20), 9181−5.
(13) Pastukhov, O.; Schwalm, S.; Zangemeister-Wittke, U.; Fabbro, D.; Bornancin, F.; Japtok, L.; Kleuser, B.; Pfeilschifter, J.; Huwiler, A. The ceramide kinase inhibitor NVP-231 inhibits breast and lung cancer cell proliferation by inducing M phase arrest and subsequent cell death. *Br. J. Pharmacol.* **2014**, *171* (24), 5829−44.
(14) Rojas, C.; Barnaeva, E.; Thomas, A. G.; Hu, X.; Southall, N.; Marugan, J.; Chaudhuri, A. D.; Yoo, S. W.; Hin, N.; Stepanek, O.; Wu, Y.; Zimmermann, S. C.; Gadiano, A. G.; Tsukamoto, T.; Rais, R.; Haughey, N.; Ferrer, M.; Slusher, B. S. DPTIP, a newly identified potent brain penetrant neutral sphingomyelinase 2 inhibitor, regulates astrocyte-peripheral immune communication following brain inflammation. *Sci. Rep* **2018**, *8* (1), 17715.
(15) Raisova, M.; Goltz, G.; Bektas, M.; Bielawska, A.; Riebeling, C.; Hossini, A. M.; Eberle, J.; Hannun, Y. A.; Orfanos, C. E.; Geilen, C. C. Bcl-2 overexpression prevents apoptosis induced by ceramidase inhibitors in malignant melanoma and HaCaT keratinocytes. *FEBS Lett.* **2002**, *516* (1−3), 47−52.
(16) Gupta, P.; Taiyab, A.; Hussain, A.; Alajmi, M. F.; Islam, A.; Hassan, M. I. Targeting the Sphingosine Kinase/Sphingosine-1-Phosphate Signaling Axis in Drug Discovery for Cancer Therapy. *Cancers (Basel)* **2021**, *13* (8), 1898.
(17) Britten, C. D.; Garrett-Mayer, E.; Chin, S. H.; Shirai, K.; Ogretmen, B.; Bentz, T. A.; Brisendine, A.; Anderton, K.; Cusack, S. L.; Maines, L. W.; Zhuang, Y.; Smith, C. D.; Thomas, M. B. A Phase I Study of ABC294640, a First-in-Class Sphingosine Kinase-2 Inhibitor, in Patients with Advanced Solid Tumors. *Clin. Cancer Res.* **2017**, *23* (16), 4642−4650.
(18) Hamada, M.; Kameyama, H.; Iwai, S.; Yura, Y. Induction of autophagy by sphingosine kinase 1 inhibitor PF-543 in head and neck squamous cell carcinoma cells. *Cell Death Discov* **2017**, *3*, 17047.
(19) Trayssac, M.; Hannun, Y. A.; Obeid, L. M. Role of sphingolipids in senescence: implication in aging and age-related diseases. *J. Clin Invest* **2018**, *128* (7), 2702−2712.
(20) Hoeferlin, L. A.; Wijesinghe, D. S.; Chalfant, C. E. The role of ceramide-1-phosphate in biological functions. *Handb Exp Pharmacol* **2013**, *215* (215), 153−66.
(21) Wijesinghe, D. S.; Subramanian, P.; Lamour, N. F.; Gentile, L. B.; Granado, M. H.; Bielawska, A.; Szulc, Z.; Gomez-Munoz, A.; Chalfant, C. E. Chain length specificity for activation of cPLA2alpha by C1P: use of the dodecane delivery system to determine lipid-specific effects. *J. Lipid Res.* **2009**, *50* (10), 1986−95.
(22) Gomez-Munoz, A.; Kong, J. Y.; Parhar, K.; Wang, S. W.; Gangoiti, P.; Gonzalez, M.; Eivemark, S.; Salh, B.; Duronio, V.; Steinbrecher, U. P. Ceramide-1-phosphate promotes cell survival through activation of the phosphatidylinositol 3-kinase/protein kinase B pathway. *FEBS Lett.* **2005**, *579* (17), 3744−50.
(23) Gomez-Munoz, A.; Kong, J. Y.; Salh, B.; Steinbrecher, U. P. Ceramide-1-phosphate blocks apoptosis through inhibition of acid sphingomyelinase in macrophages. *J. Lipid Res.* **2004**, *45* (1), 99−105.
(24) Granado, M. H.; Gangoiti, P.; Ouro, A.; Arana, L.; Gomez-Munoz, A. Ceramide 1-phosphate inhibits serine palmitoyltransferase and blocks apoptosis in alveolar macrophages. *Biochim. Biophys. Acta* **2009**, *1791* (4), 263−72.
(25) Pettus, B. J.; Bielawska, A.; Subramanian, P.; Wijesinghe, D. S.; Maceyka, M.; Leslie, C. C.; Evans, J. H.; Freiberg, J.; Roddy, P.; Hannun, Y. A.; Chalfant, C. E. Ceramide 1-phosphate is a direct activator of cytosolic phospholipase A2. *J. Biol. Chem.* **2004**, *279* (12), 11320−6.
(26) Coppe, J. P.; Desprez, P. Y.; Krtolica, A.; Campisi, J. The senescence-associated secretory phenotype: the dark side of tumor suppression. *Annu. Rev. Pathol* **2010**, *5*, 99−118.
(27) Pettus, B. J.; Bielawska, A.; Spiegel, S.; Roddy, P.; Hannun, Y. A.; Chalfant, C. E. Ceramide kinase mediates cytokine- and calcium ionophore-induced arachidonic acid release. *J. Biol. Chem.* **2003**, *278* (40), 38206−13.
(28) Parisi, L. R.; Li, N.; Atilla-Gokcumen, G. E. Very Long Chain Fatty Acids Are Functionally Involved in Necroptosis. *Cell Chem. Biol.* **2017**, *24* (12), 1445−1454.

https://doi.org/10.1021/acschembio.2c00216
ACS Chem. Biol. 2022, 17, 822−828